Electronic Supplementary Material (ESI) for Dalton Transactions.

Supplementary Data

Modular synthesis of antimalarial quinoline-based PGM metallarectangles

Taryn M. Golding [a], Mziyanda Mbaba [a], and Gregory S. Smith [a,*]

[a] *Department of Chemistry, University of Cape Town, Rondebosch, Cape Town, South Africa*

*Corresponding authors' E-mail address: gregory.smith@uct.ac.za

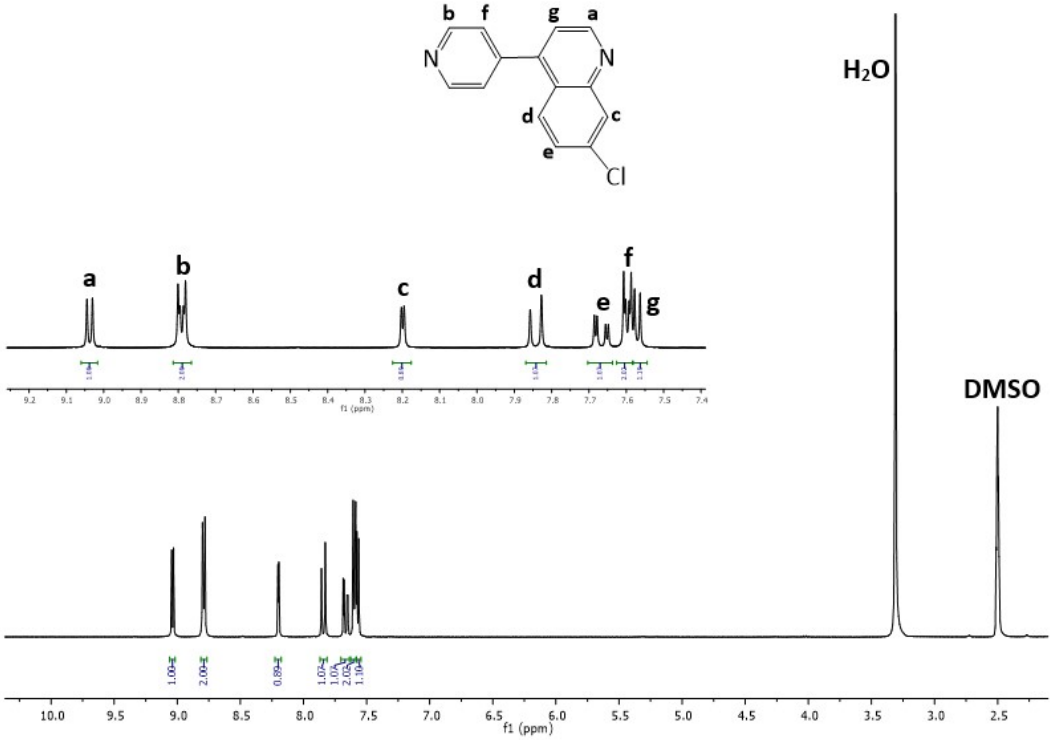

Fig. S1 ^{1}H NMR spectrum of ligand **L** in DMSO.

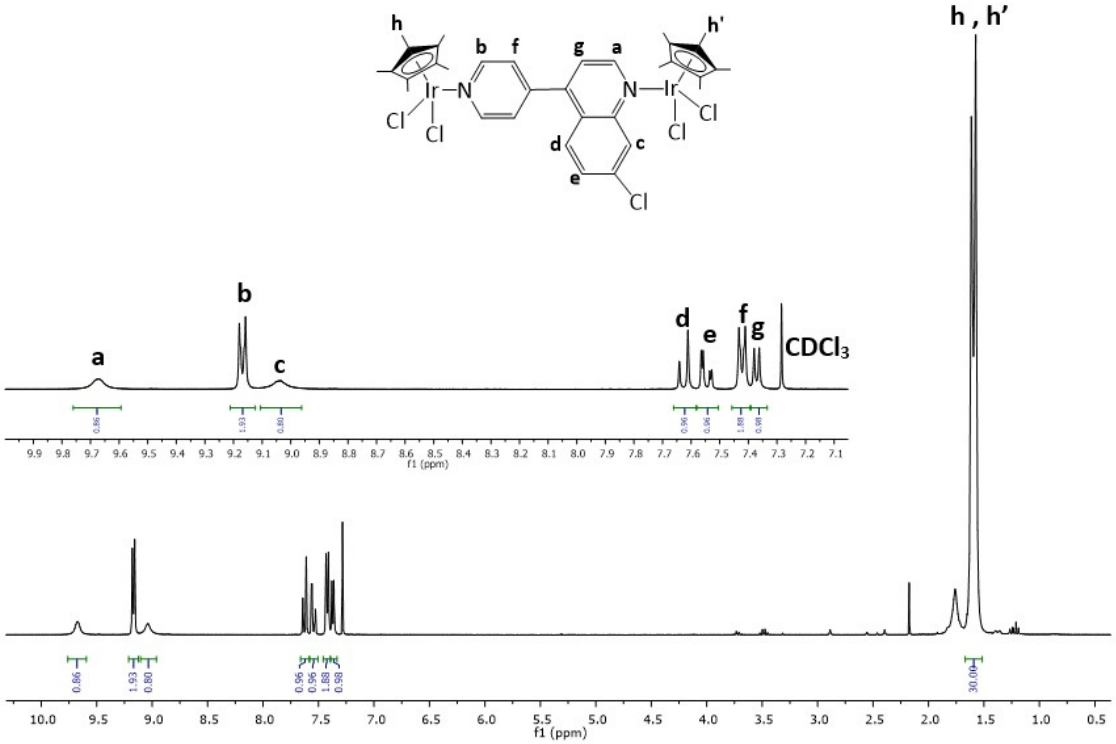

Fig. S2 ^{1}H NMR spectrum of binuclear complex **1c** in $CDCl_3$.

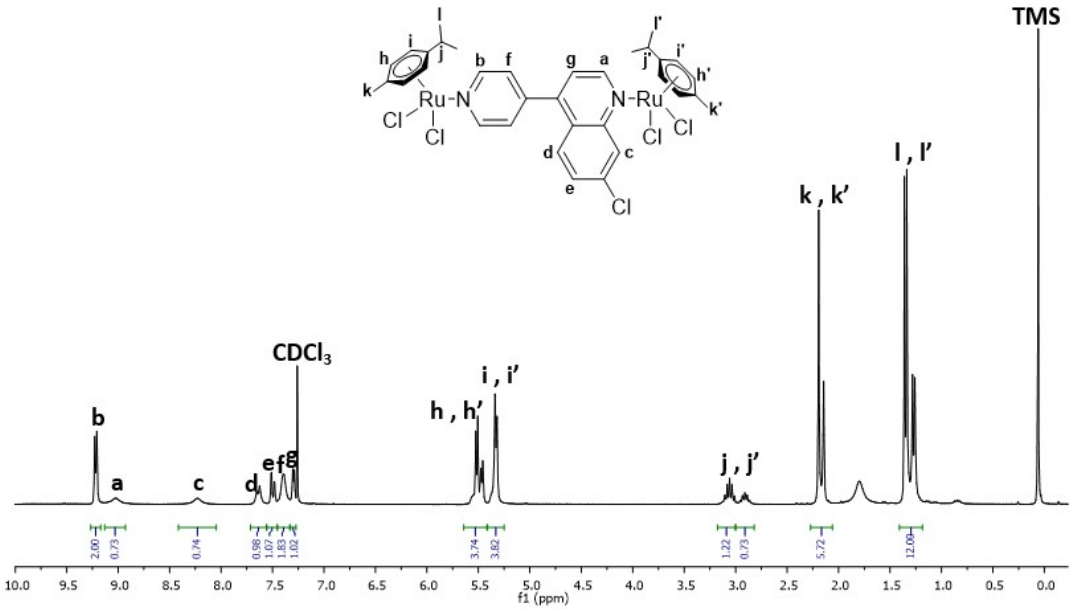

Fig. S3 ^{1}H NMR spectrum of binuclear complex **1d** in $CDCl_3$.

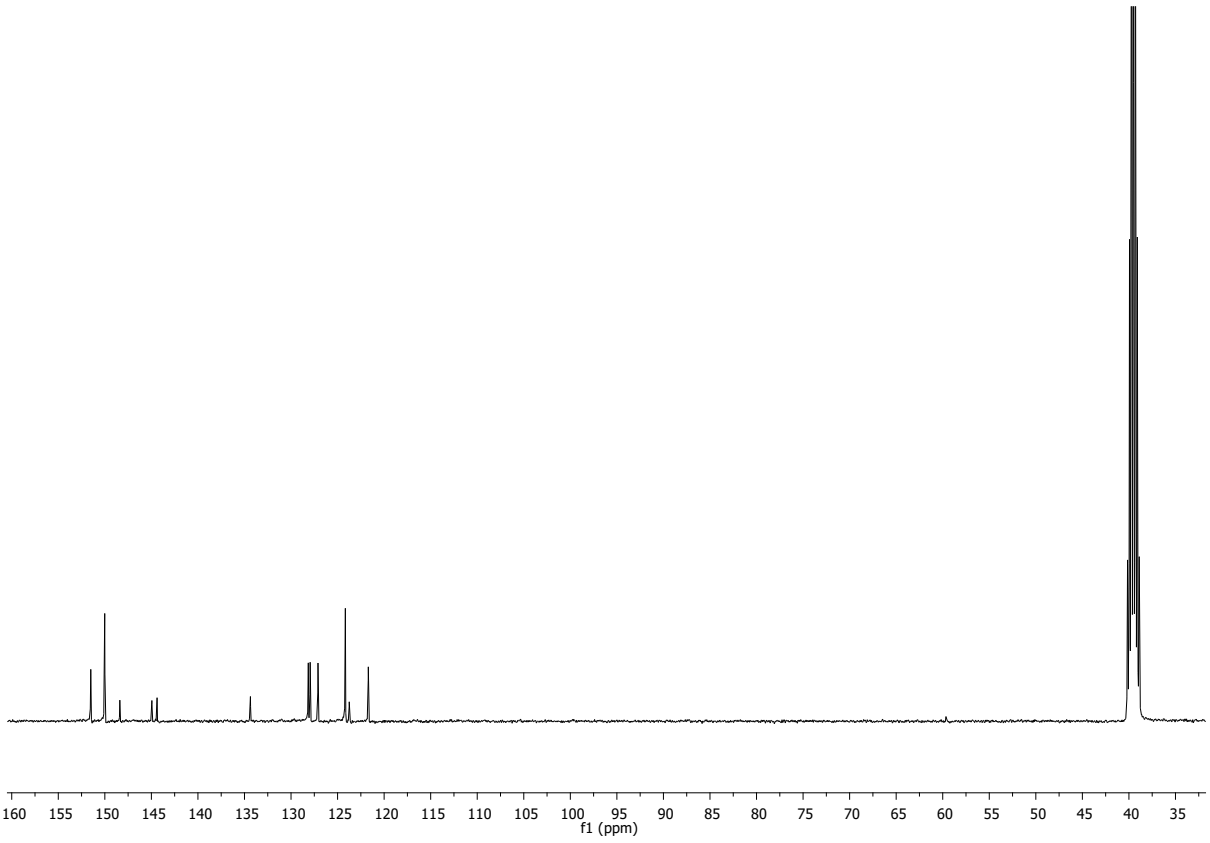

Fig. S4 $^{13}C\{^{1}H\}$ NMR spectrum of ligand **L** in DMSO.

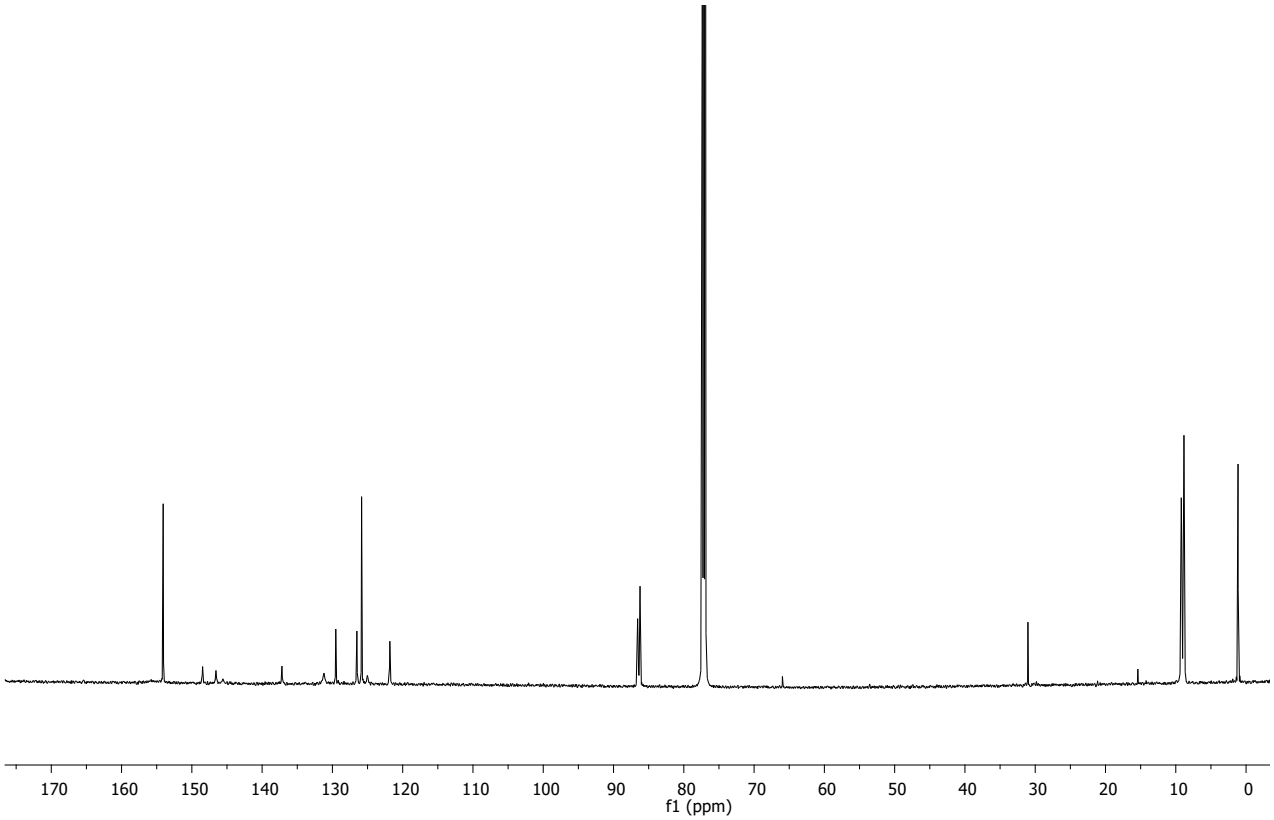

Fig. S5 $^{13}C\{^{1}H\}$ NMR spectrum of binuclear complex **1c** in $CDCl_3$.

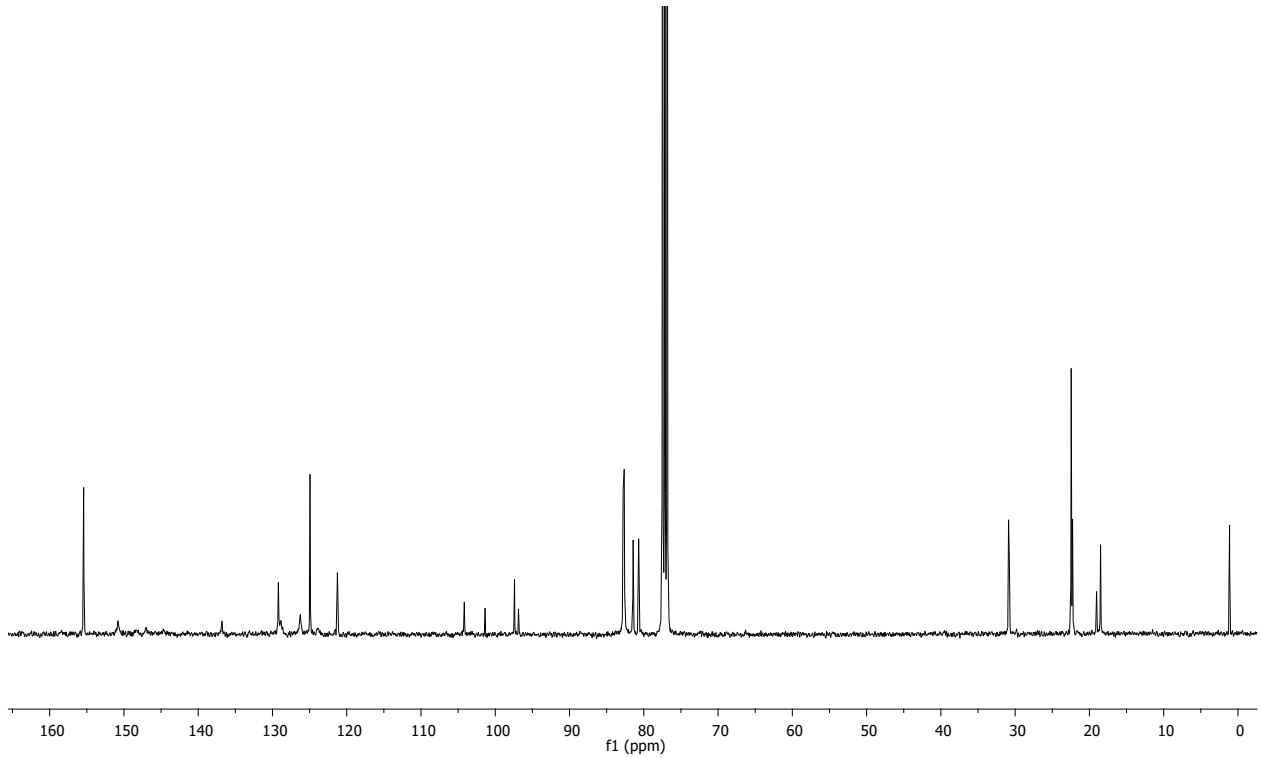

Fig. S6 $^{13}C\{^{1}H\}$ NMR spectrum of binuclear complex **1d** in $CDCl_3$.

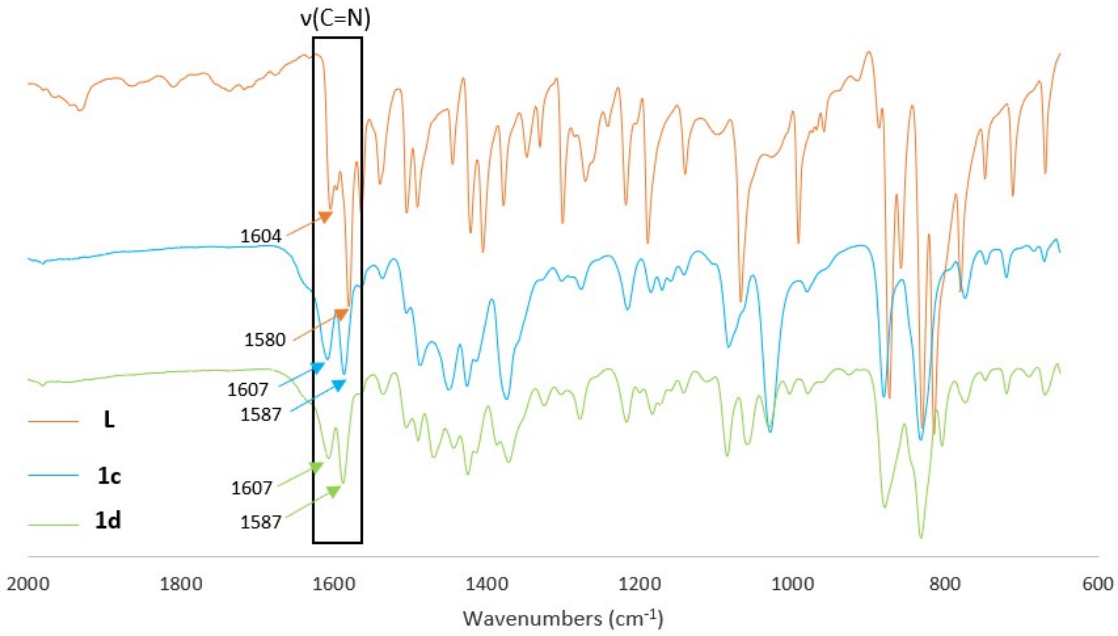

Fig. S7 Stacked IR spectra of ligand **L** and binuclear complexes **1c** and **1d**.

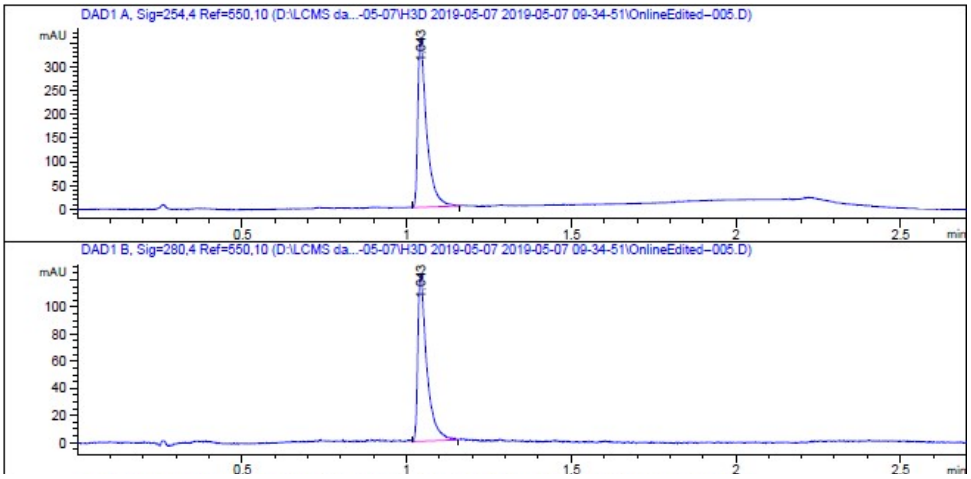

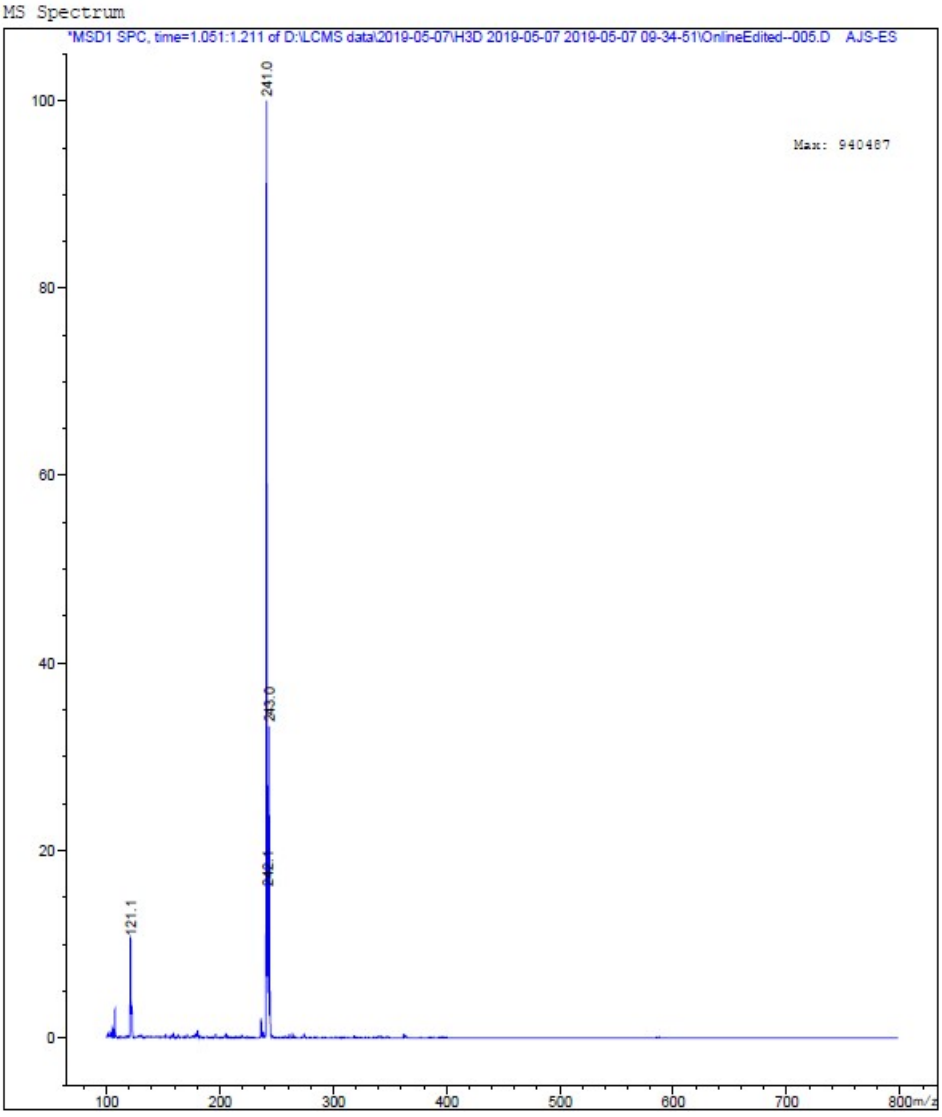

Fig. S8 LC-MS data of ligand **L**.

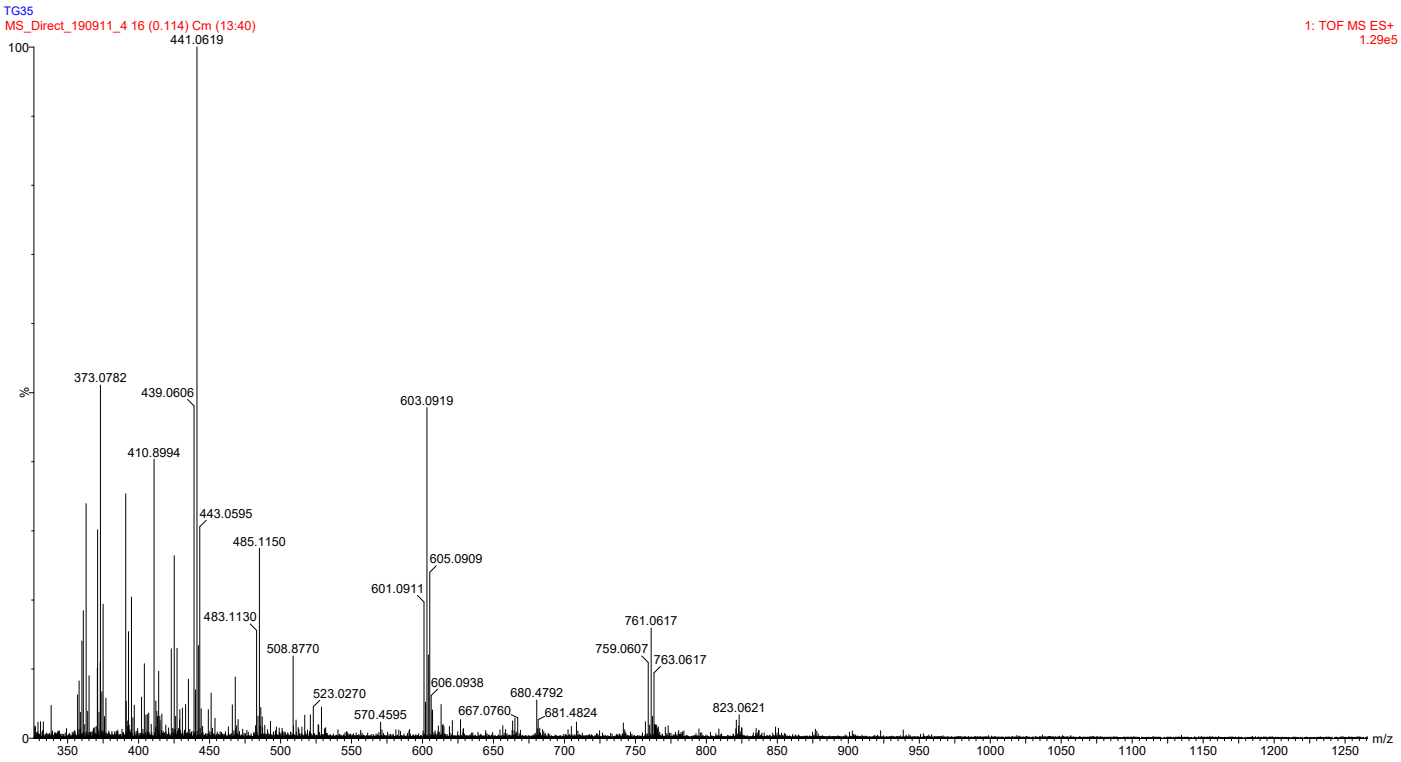

Fig. S9 Mass spectrum of binuclear complex **1c**.

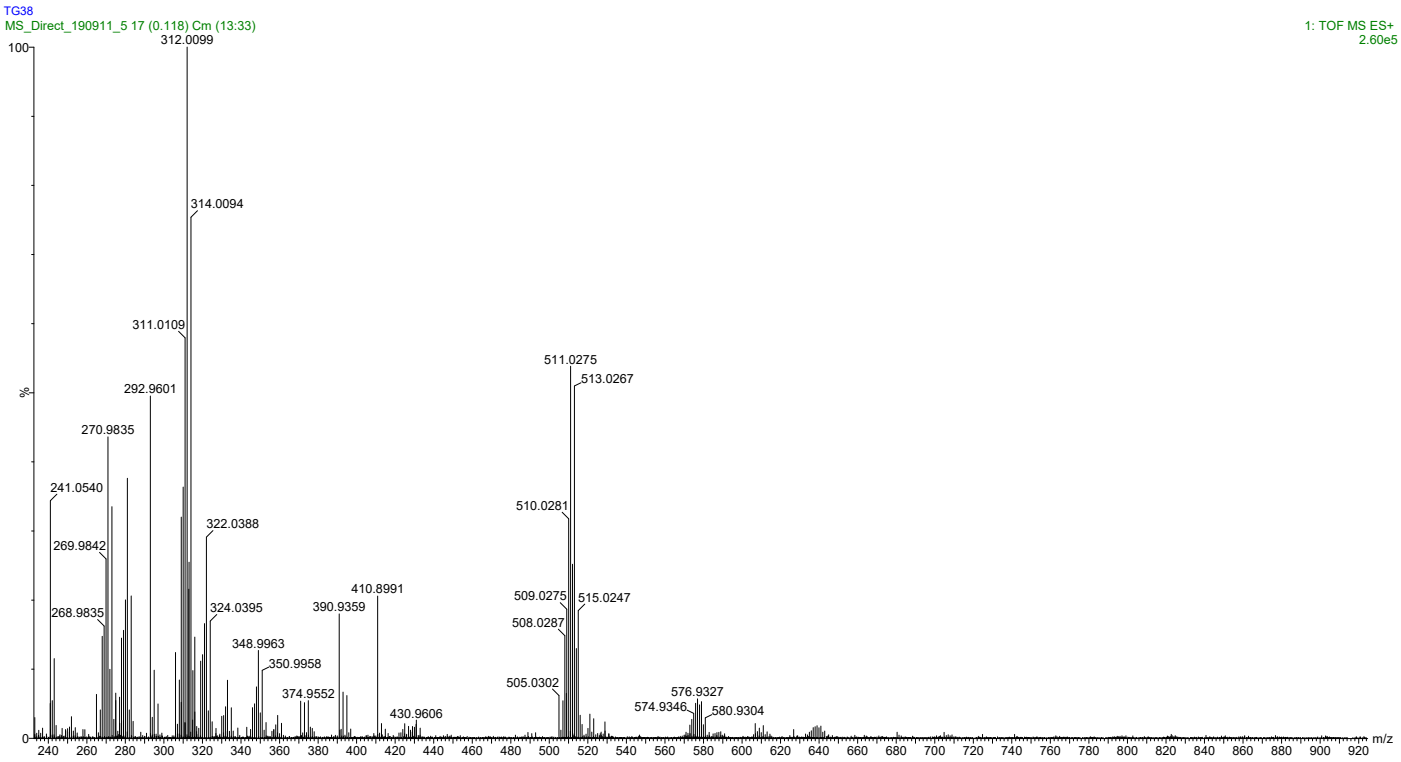

Fig. S10 Mass spectrum of binuclear complex **1d**.

Table S1 Crystallographic data and refinement parameters for complex **1c** · $5CHCl_3$.

Formula Unit	$C_{34}H_{39}Cl_5Ir_2N_2 \cdot 5(CHCl_3)$	**F(000)**	1572
Formula Weight	1634.20	**Crystal Size (mm)**	0.06 x 0.08 x 0.11
Crystal System	Triclinic	**Temperature (K)**	100
Space Group	P-1	**Scan Range (°)**	1.6 < θ < 28.3
a, b, c (Å)	11.6063 (2), 16.2300 (3), 16.3533 (3)	**Unique Reflections**	13844
α, β, γ (°)	69.543 (3), 81.622 (3), 76.793 (4)	**R_{int}**	0.102
Volume ($Å^3$)	2802.4 (9)	**Observed Data [I>2σ(I)]**	9029
Z	2	**R, wR2**	0.0548, 0.1271
Density$_{calc}$ (g/cm^3)	1.937	**Goodness-of-fit**	0.99
μ (mm^{-1})	5.729	**Min, Max Δρ ($e.Å^{-3}$)**	-1.75, 2.17

Table S2 Selected bond lengths (Å) and angles (°) for complex **1c** · $5CHCl_3$.

Bond lengths (Å)					
$Ir_1 – N_1$	2.113 (6)	**$Ir_{2A} – N_2$**	2.203 (10)	**$Ir_{2B} – N_2$**	2.147 (13)
$Ir_1 – Cl_1$	2.401 (2)	**$Ir_{2A} – Cl_3$**	2.322 (7)	**$Ir_{2B} – Cl_3$**	2.562 (10)
$Ir_1 – Cl_2$	2.417 (2)	**$Ir_{2A} – Cl_4$**	2.408 (8)	**$Ir_{2B} – Cl_4$**	2.443 (11)
$Ir_1 – C_{21}$	2.132 (8)	**$Ir_{2A} – C_{31}$**	2.170 (2)	**$Ir_{2B} – C_{41}$**	2.140 (3)
$Ir_1 – C_{22}$	2.152 (8)	**$Ir_{2A} – C_{32}$**	2.218 (19)	**$Ir_{2B} – C_{42}$**	2.170 (3)
$Ir_1 – C_{23}$	2.141 (8)	**$Ir_{2A} – C_{33}$**	2.177 (19)	**$Ir_{2B} – C_{43}$**	2.130 (5)
$Ir_1 – C_{24}$	2.155 (8)	**$Ir_{2A} – C_{34}$**	2.170 (2)	**$Ir_{2B} – C_{44}$**	2.110 (3)
$Ir_1 – C_{25}$	2.173 (8)	**$Ir_{2A} – C_{35}$**	2.170 (2)	**$Ir_{2B} – C_{45}$**	2.080 (3)
Bond angles (°)					
$Cl_1 – Ir_1 – N_1$	87.27 (18)	**$Cl_3 – Ir_{2A} – N_2$**	90.4 (3)	**$Cl_3 – Ir_{2B} – N_2$**	85.5 (4)
$Cl_2 – Ir_1 – N_1$	86.9 (2)	**$Cl_4 – Ir_{2A} – N_2$**	88.7 (3)	**$Cl_4 – Ir_{2B} – N_2$**	89.0 (4)
$Cl_1 – Ir_1 – Cl_2$	87.64 (7)	**$Cl_3 – Ir_{2A} – Cl_4$**	89.1 (2)	**$Cl_3 – Ir_{2B} – Cl_4$**	83.0 (3)

Torsion angle (°)	
$C_2 – C_3 – C_6 – C_7$	44.3 (12)

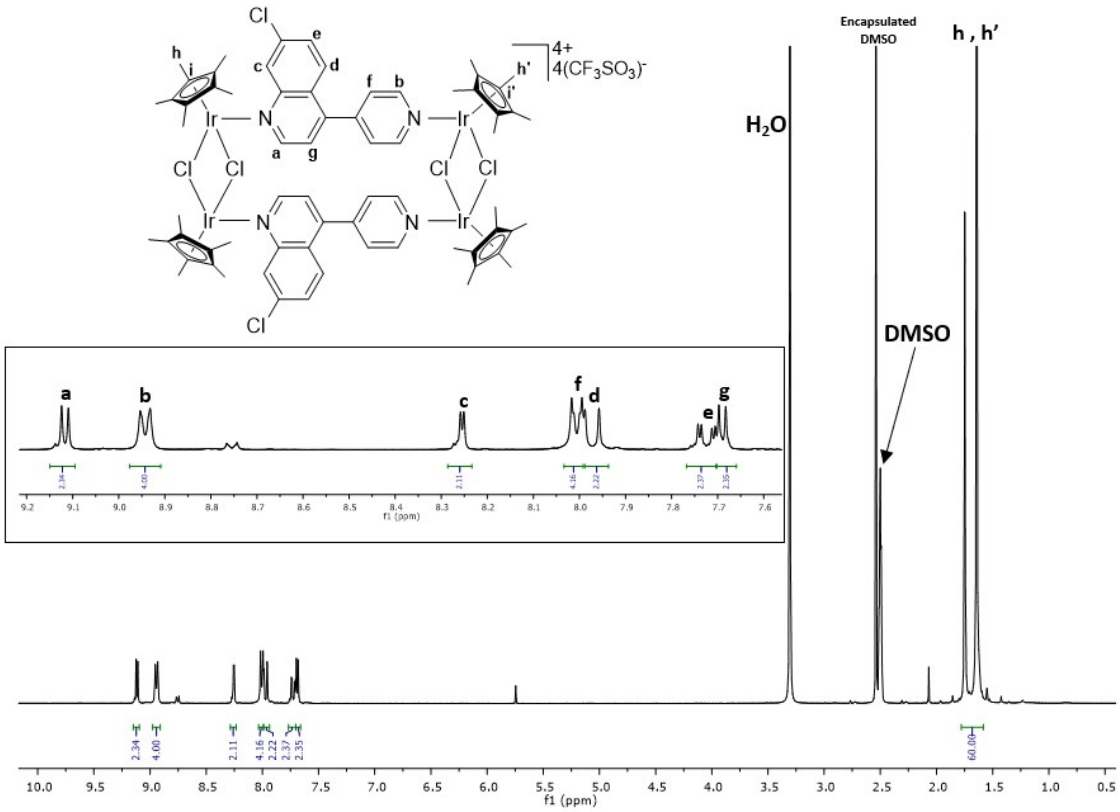

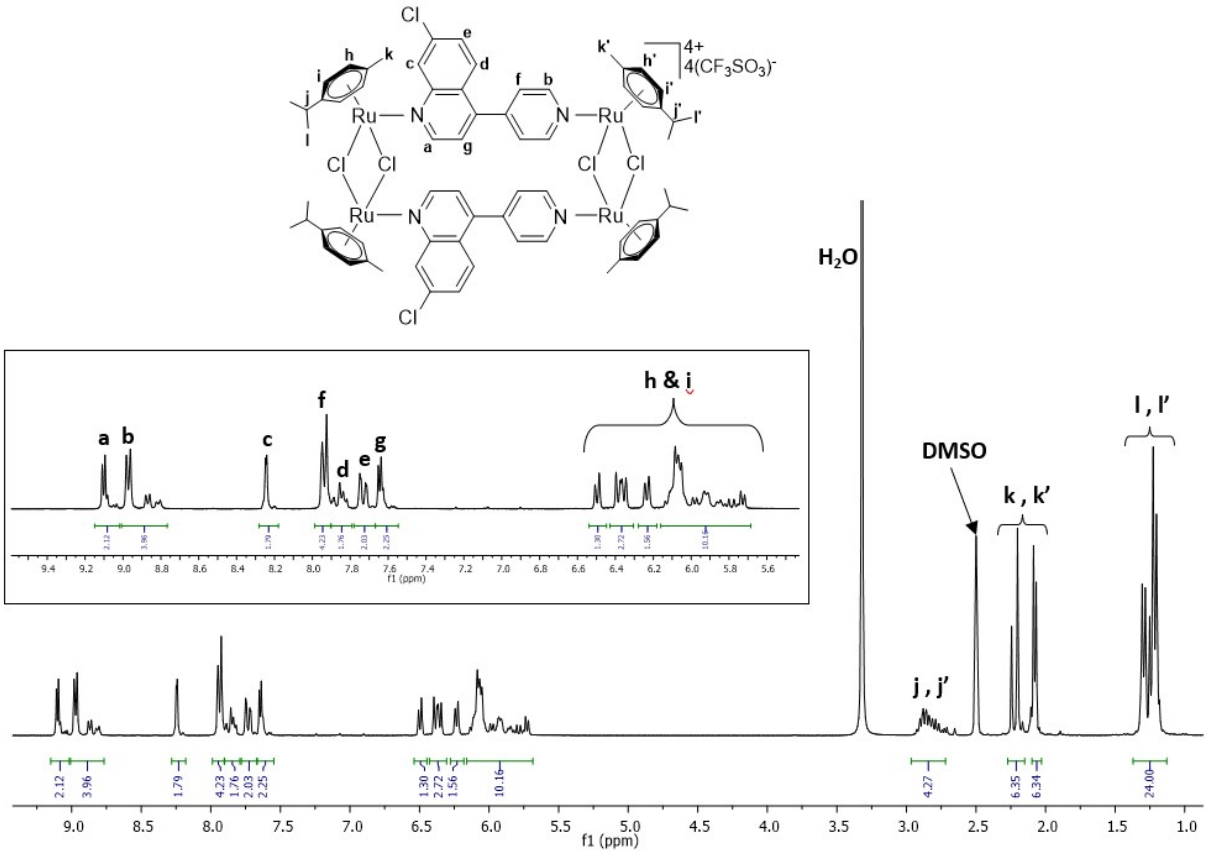

Fig. S11 ^{1}H NMR spectrum of metallarectangle **2c** in DMSO.

Fig. S12 ^{1}H NMR spectrum of metallarectangle **2d** in DMSO.

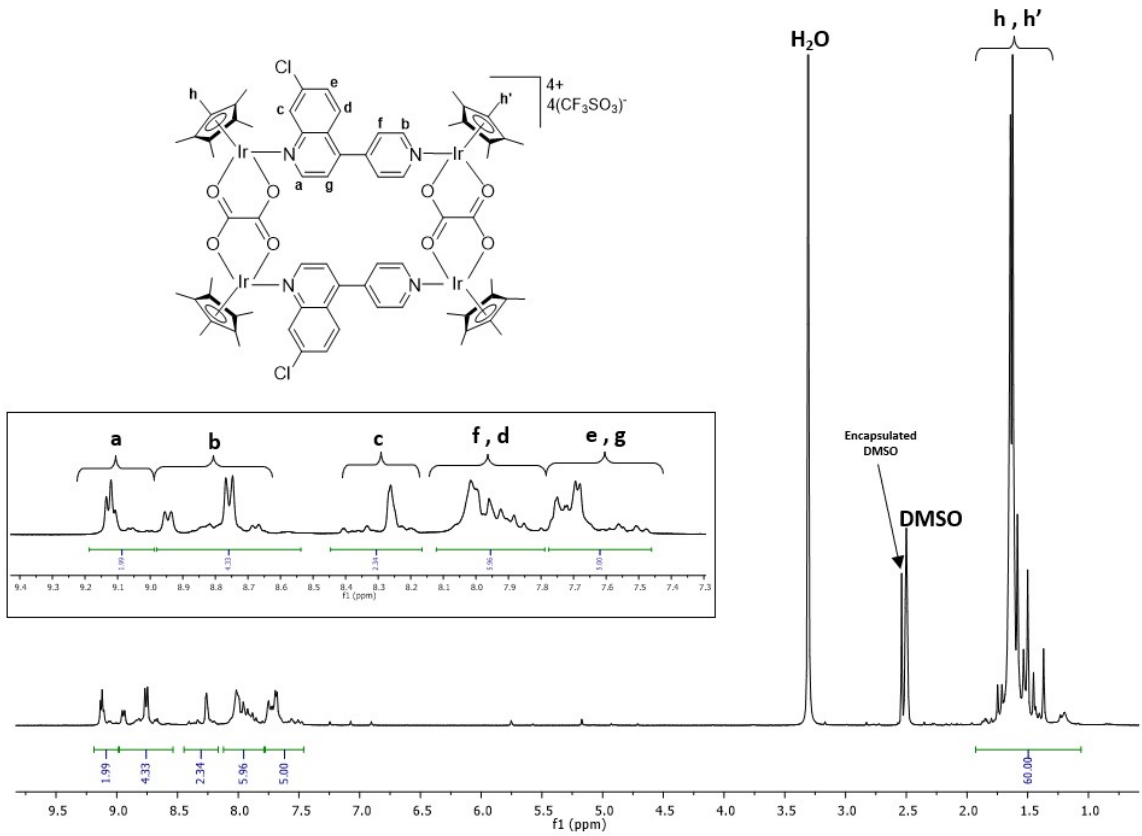

Fig. S13 ^{1}H NMR spectrum of metallarectangle **3c** in DMSO.

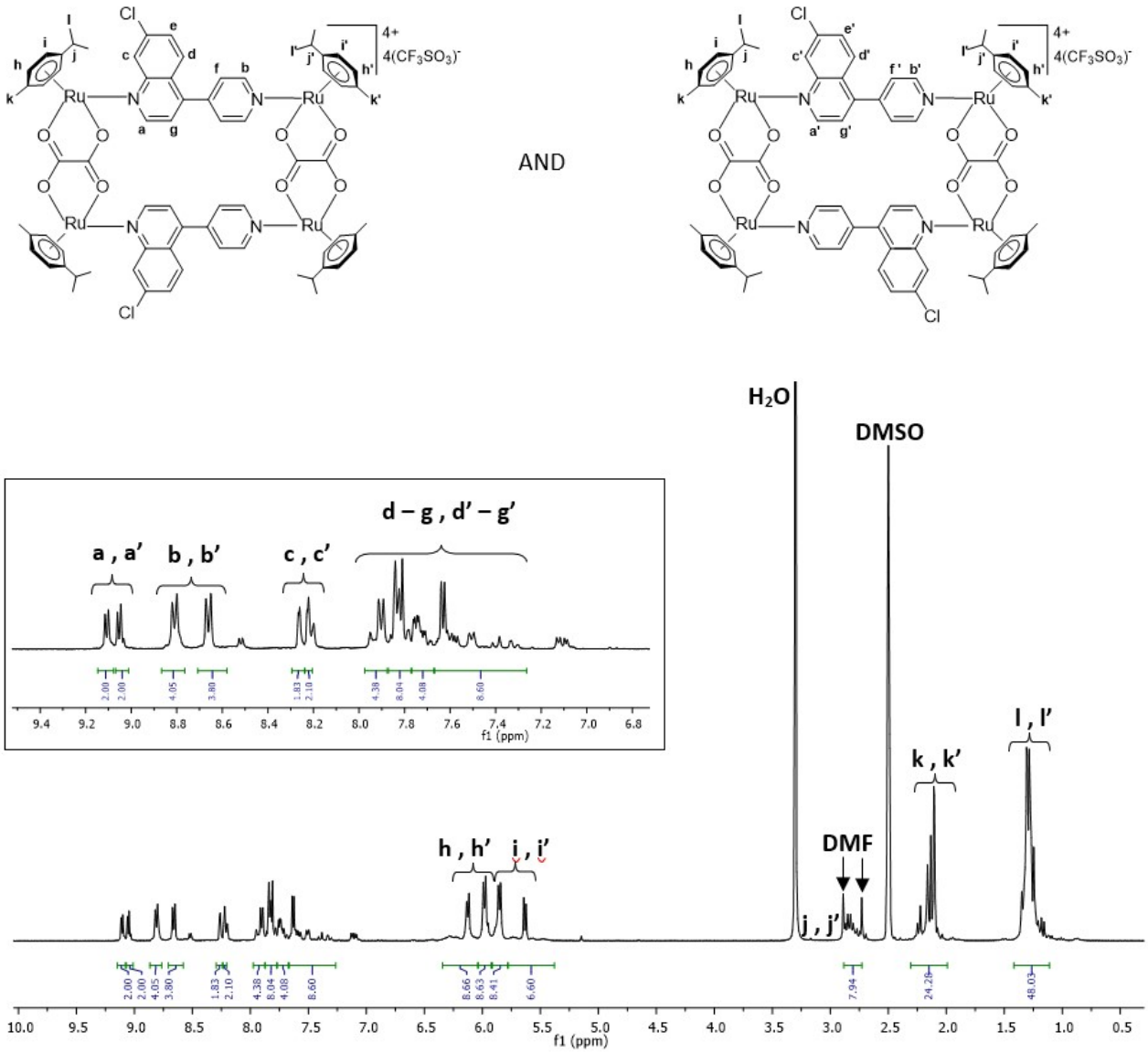

Fig. S14 ^{1}H NMR spectrum of metallarectangle **3d** in DMSO.

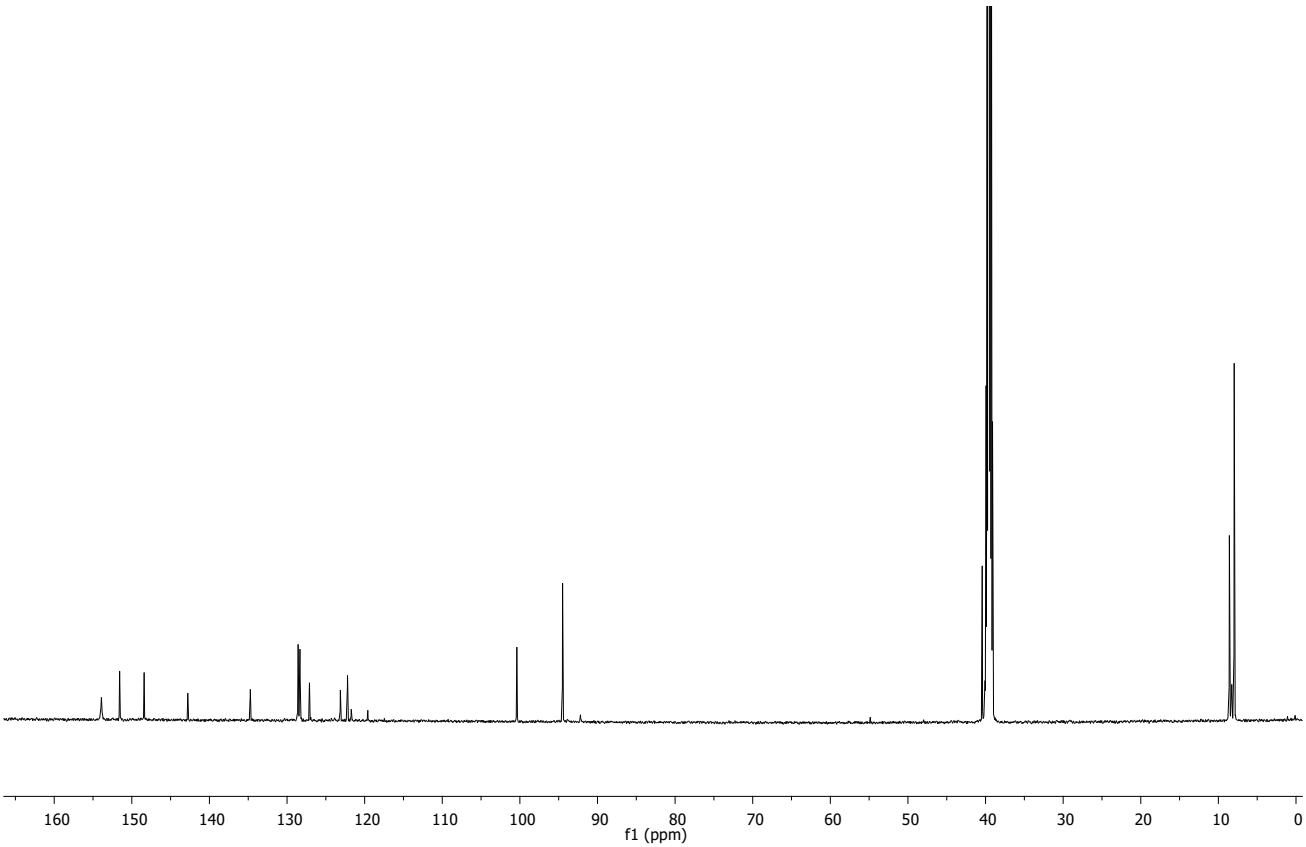

Fig. S15 $^{13}C\{^{1}H\}$ NMR spectrum of metallarectangle **2c** in DMSO.

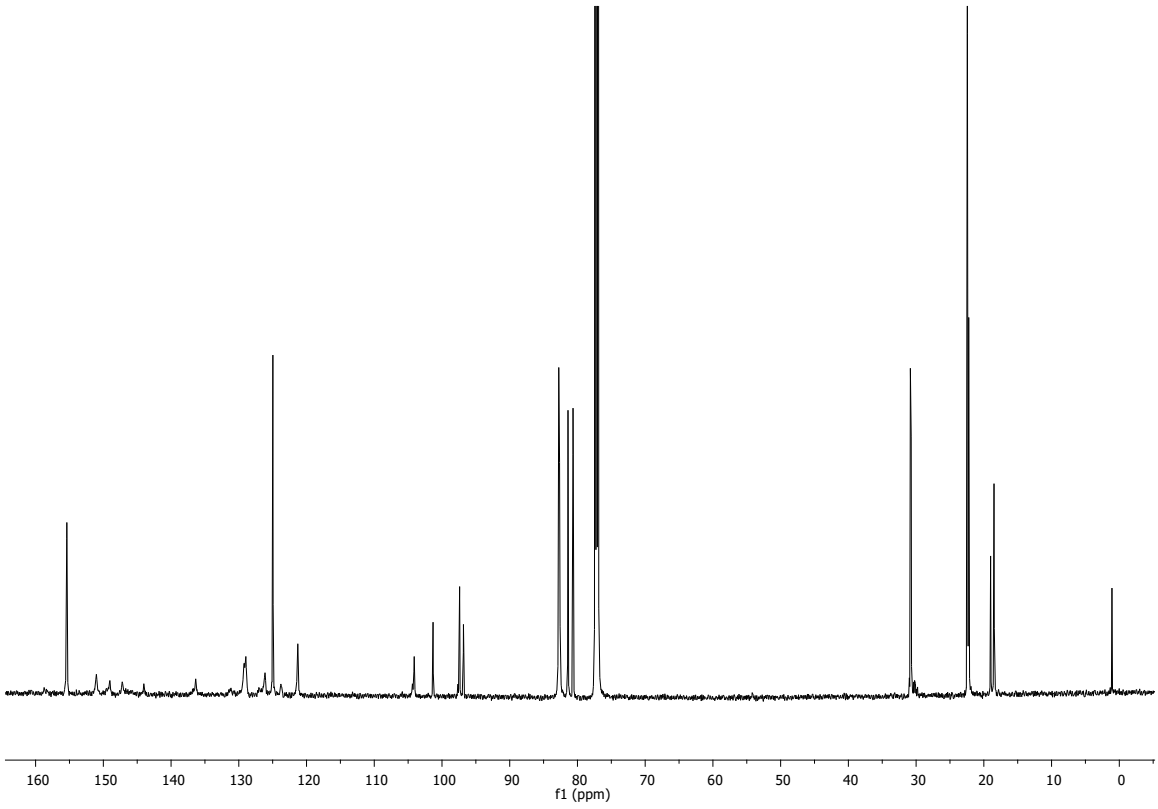

Fig. S16 $^{13}C\{^{1}H\}$ NMR spectrum of metallarectangle **2d** in DMSO.

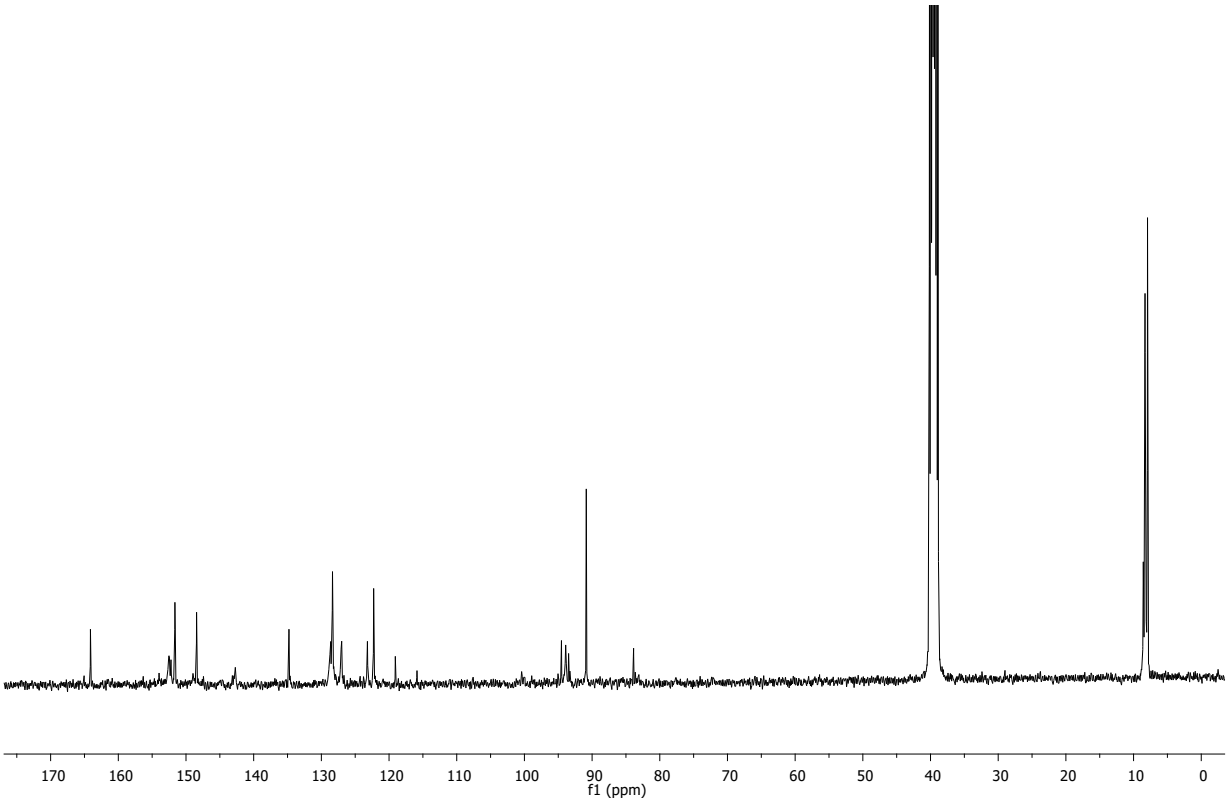

Fig. S17 $^{13}C\{^{1}H\}$ NMR spectrum of metallarectangle **3c** in DMSO.

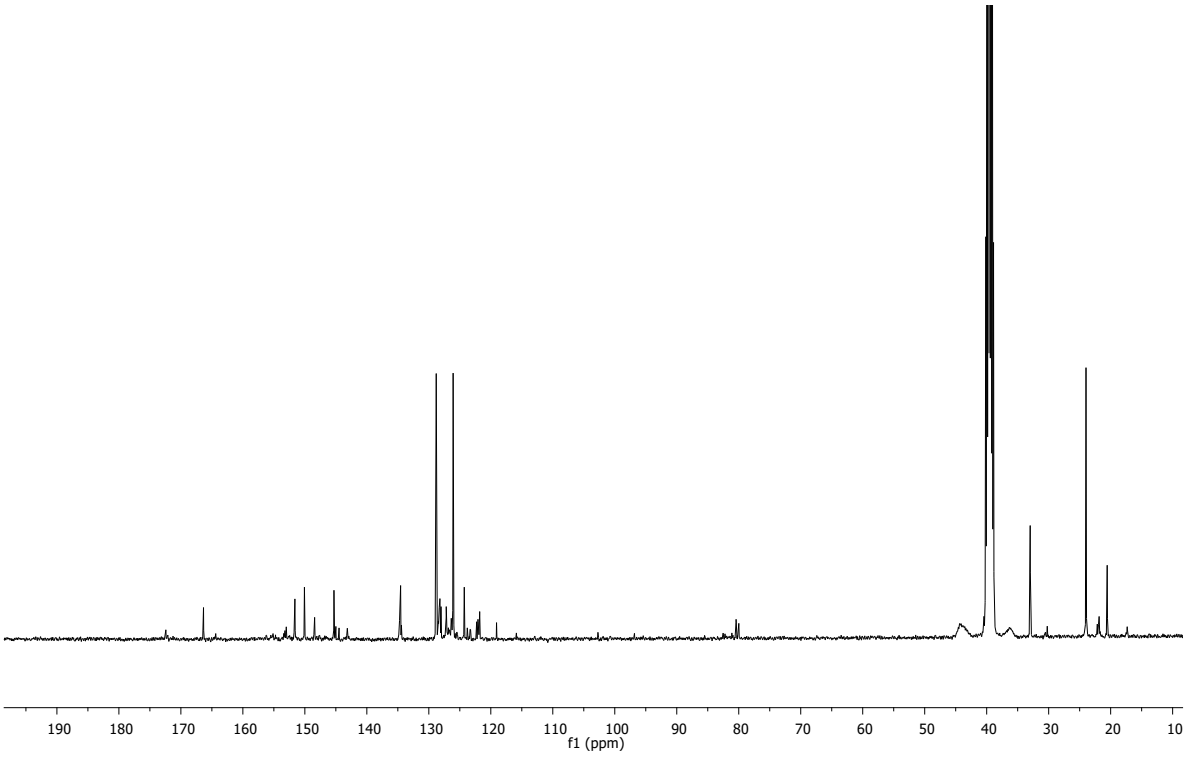

Fig. S18 $^{13}C\{^{1}H\}$ NMR spectrum of metallarectangle **3d** in DMSO.

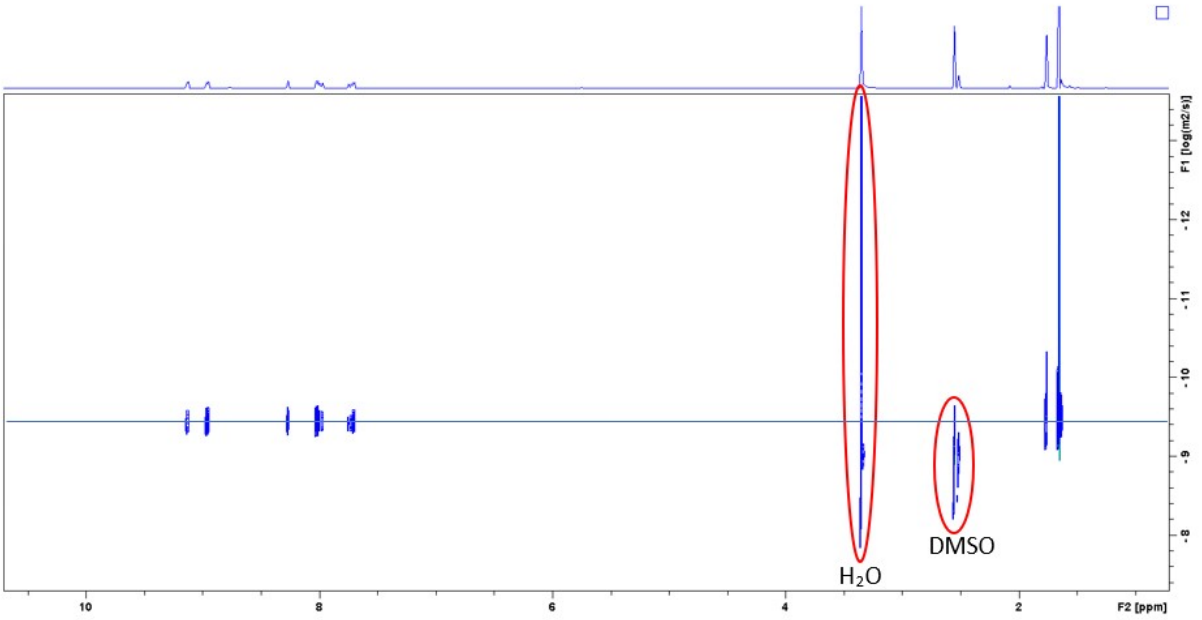

Fig. S19 DOSY NMR spectrum of metallarectangle **2c** in DMSO.

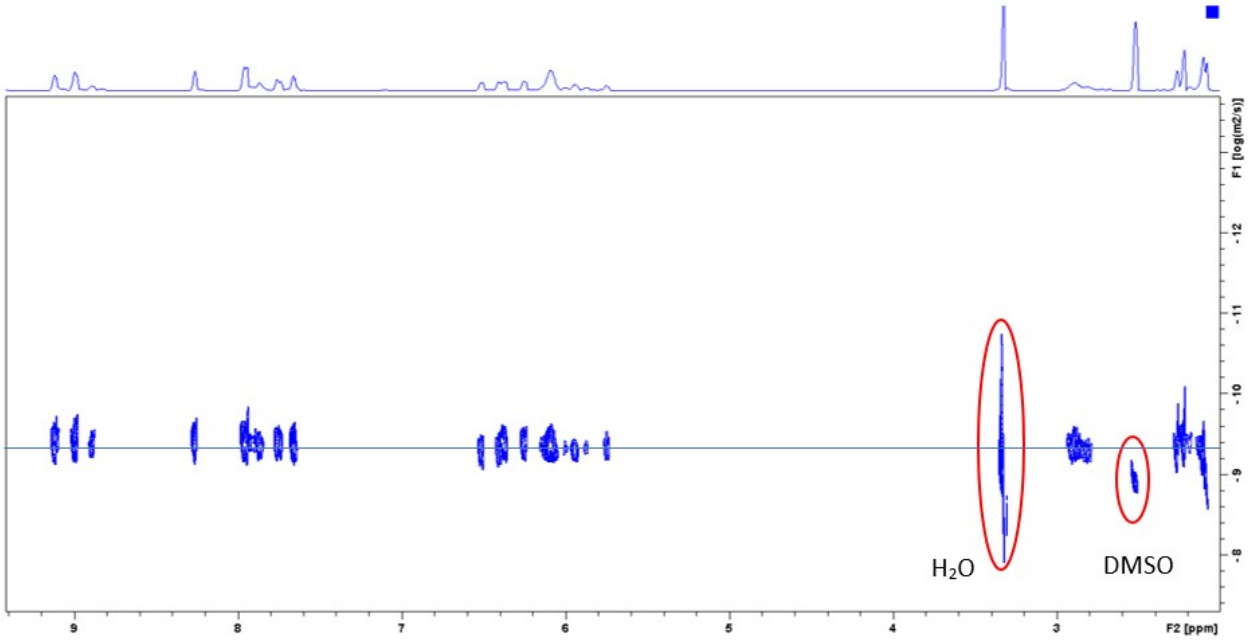

Fig. S20 DOSY NMR spectrum of metallarectangle **2d** in DMSO.

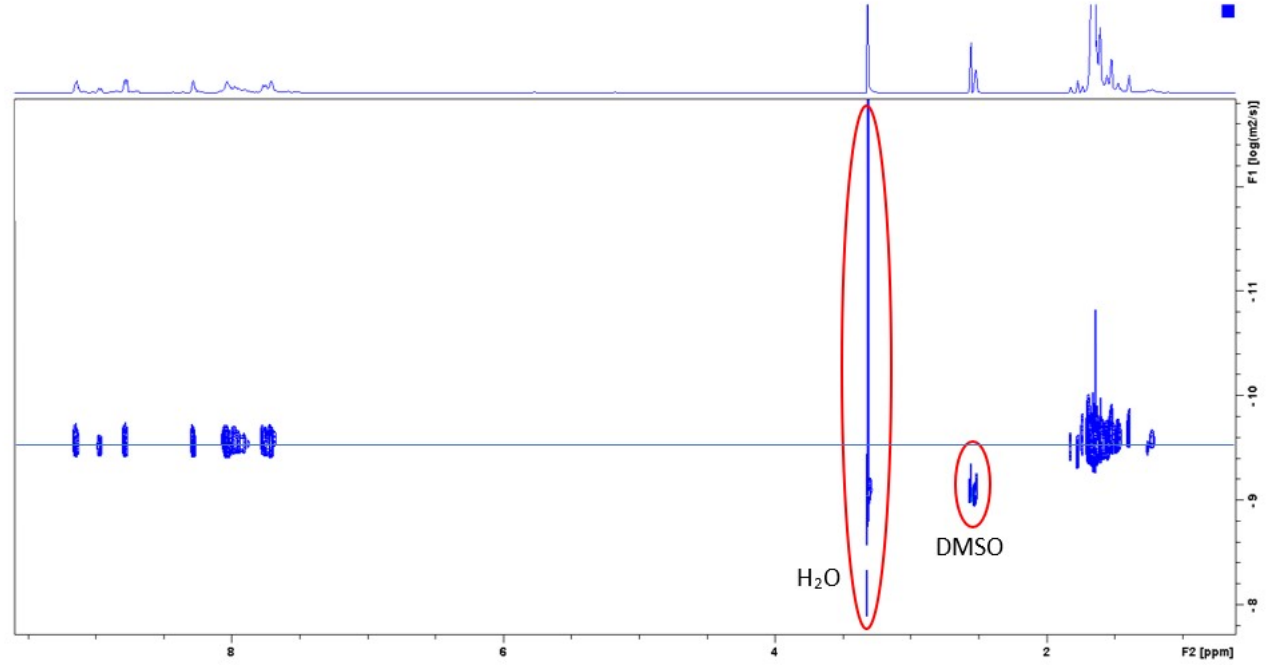

Fig. S21 DOSY NMR spectrum of metallarectangle **3c** in DMSO.

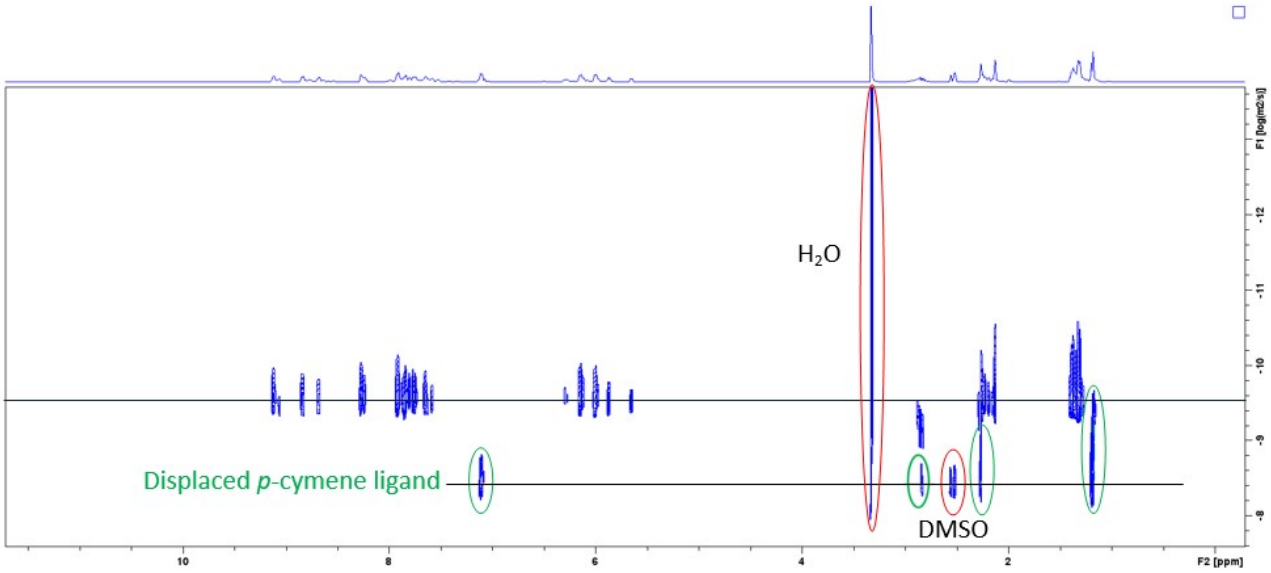

Fig. S22 DOSY NMR spectrum of metallarectangle **3d** in DMSO.

Note: Displaced *p*-cymene ligand is due to the NMR sample standing too long before being analyzed.

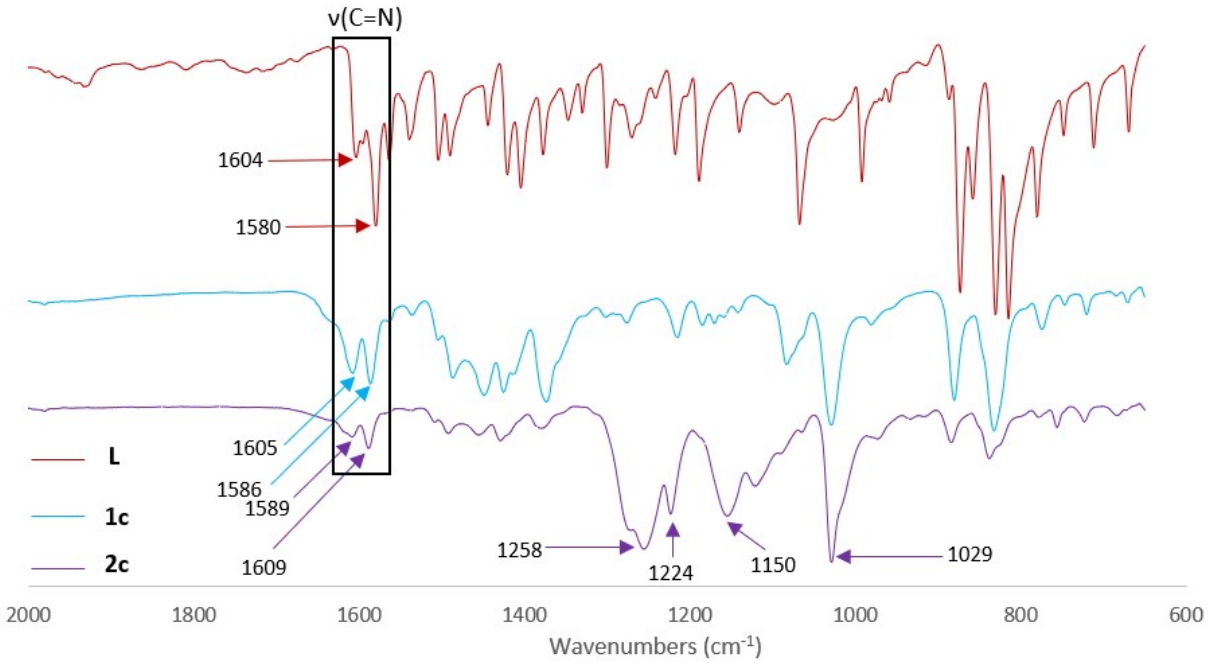

Fig. S23 Stacked IR spectra of ligand **L**, binuclear complex **1c**, and metallarectangle **2c**.

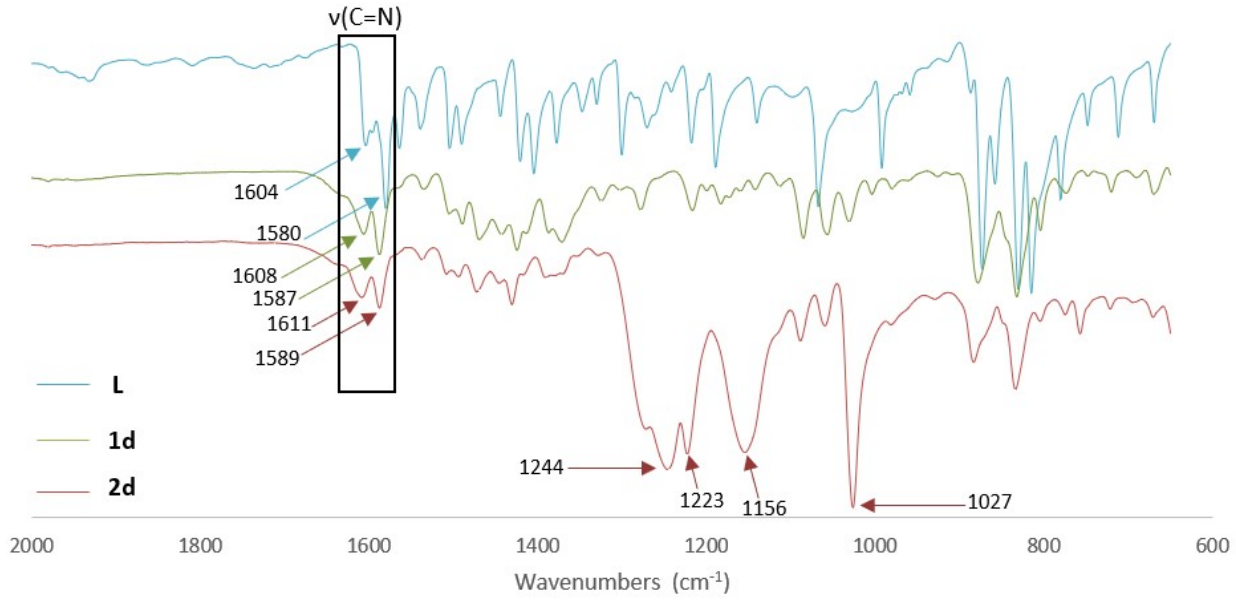

Fig. S24 Stacked IR spectra of ligand **L**, binuclear complex **1d**, and metallarectangle **2d**.

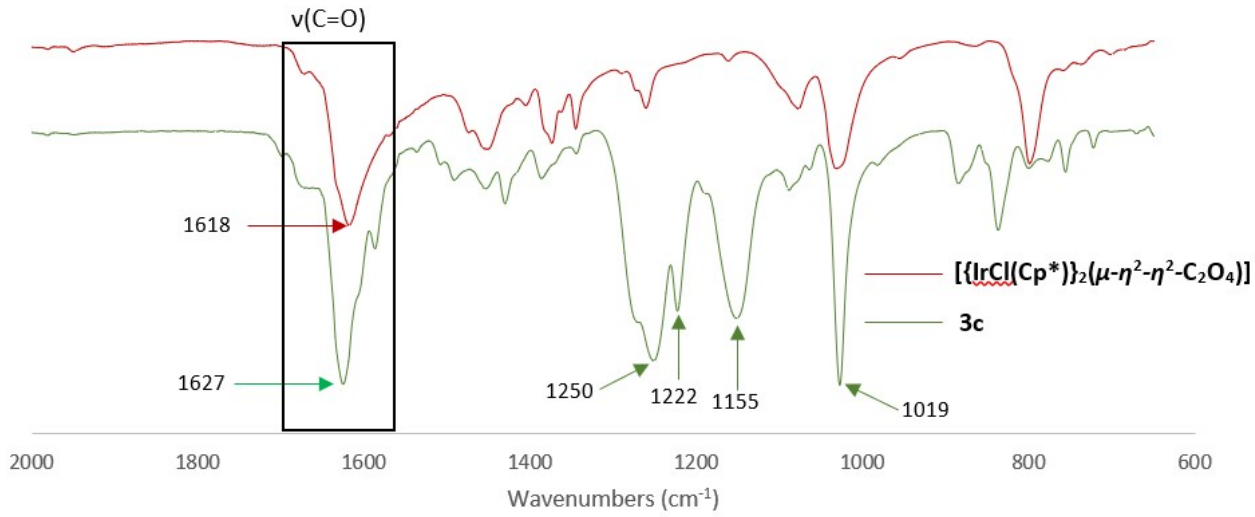

Fig. S25 Stacked IR spectra of [{IrCl(Cp*)}$_2$(μ-η^2-η^2-C_2O_4)] and metallarectangle **3c**.

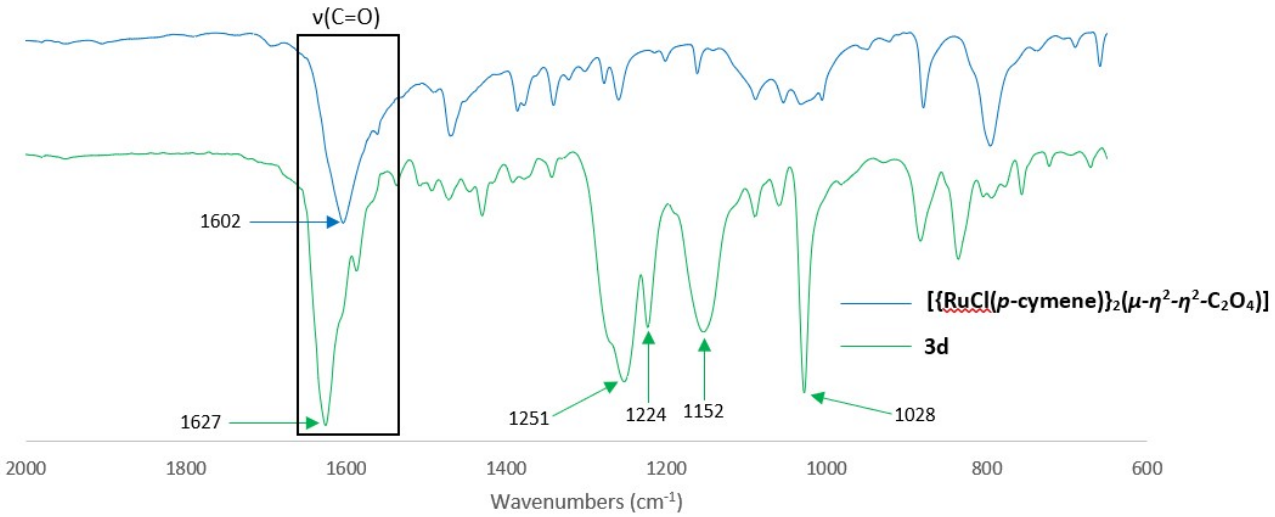

Fig. S26 Stacked IR spectra of [{RuCl(*p*-cymene)}$_2$(μ-η^2-η^2-C_2O_4)] and metallarectangle **3d**.

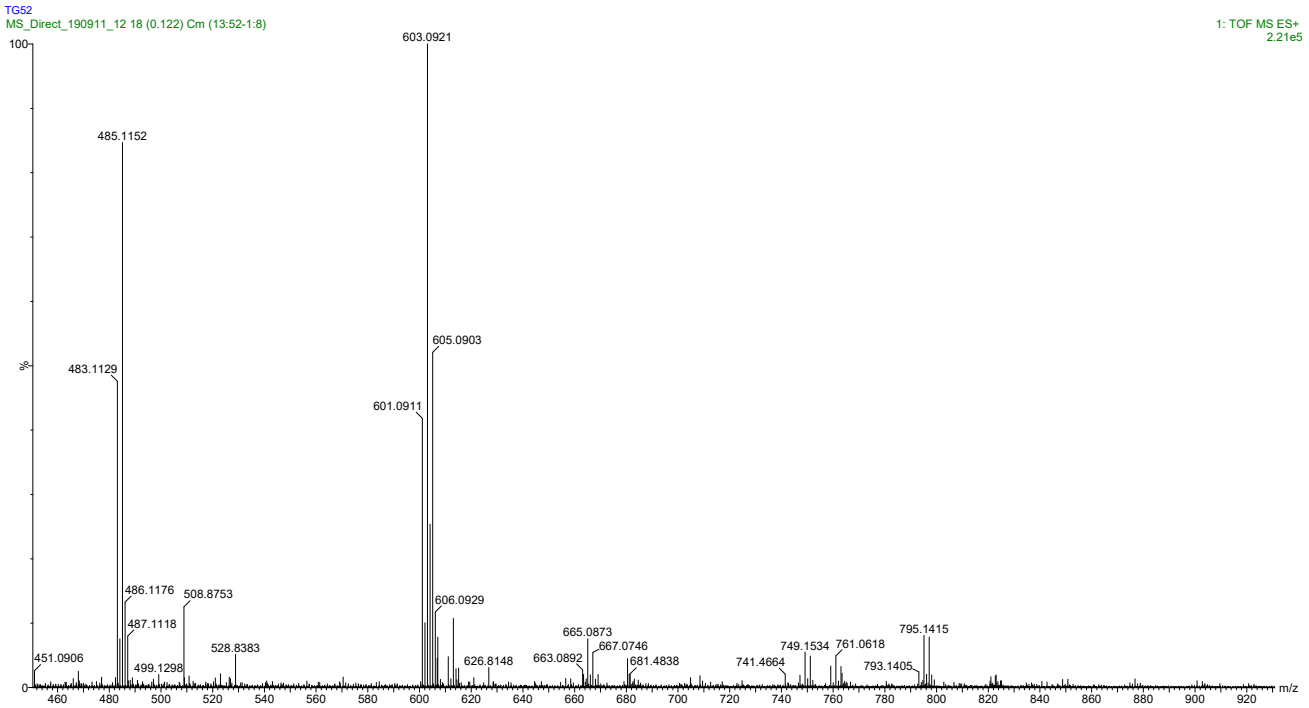

Fig. S27 Mass spectrum of metallarectangle **2c**.

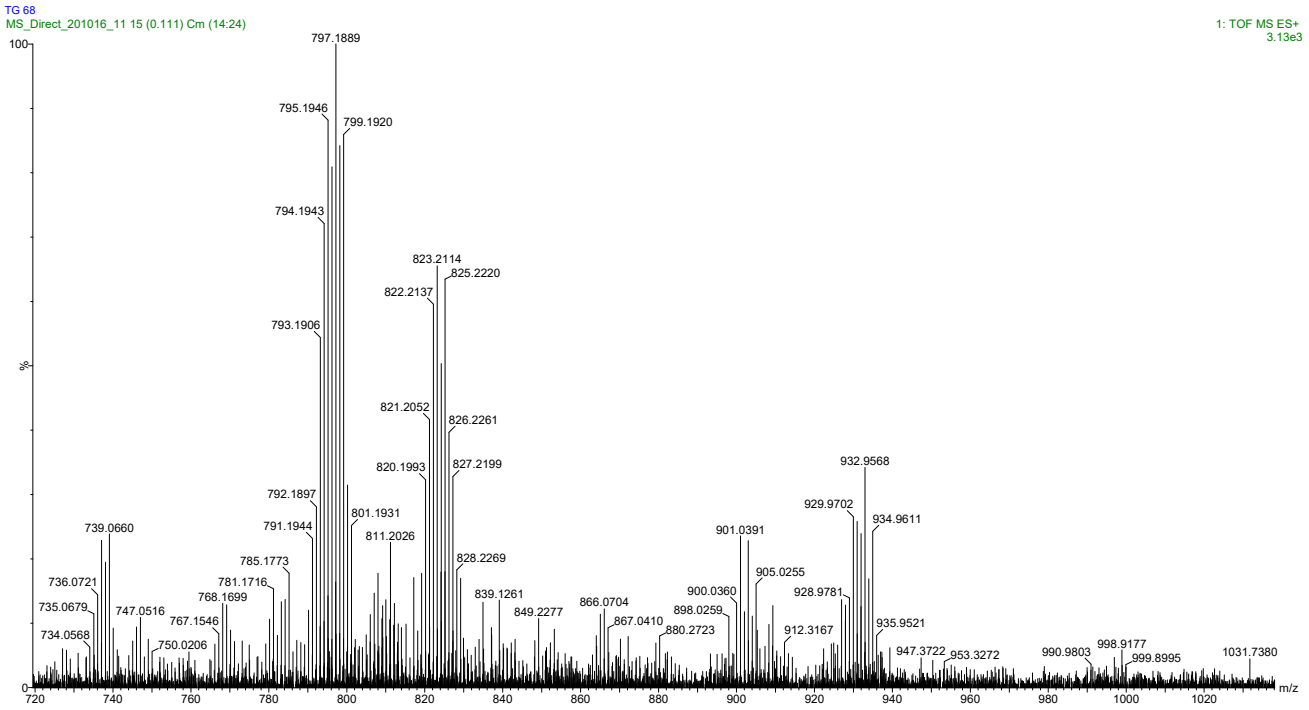

Fig. S28 Mass spectrum of metallarectangle **2d**.

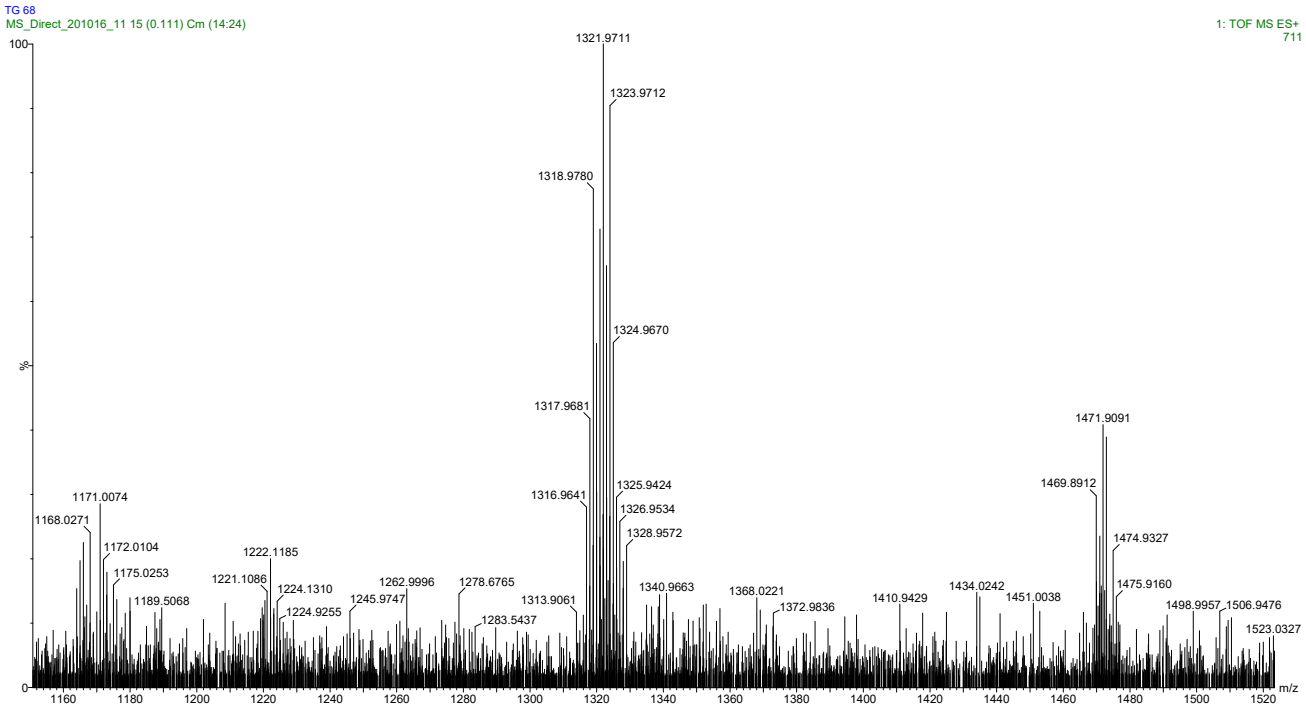

Fig. S29 Mass spectrum of metallarectangle **2d**.

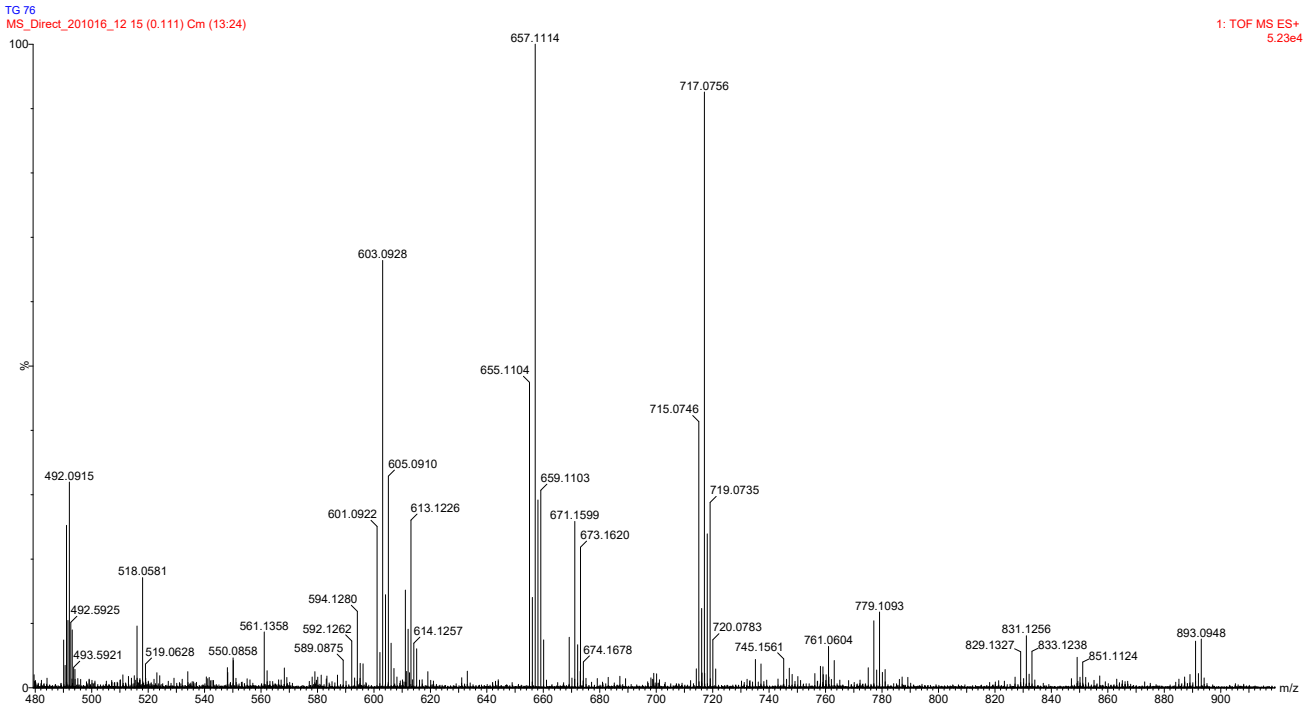

Fig. S30 Mass spectrum of metallarectangle **3c**.

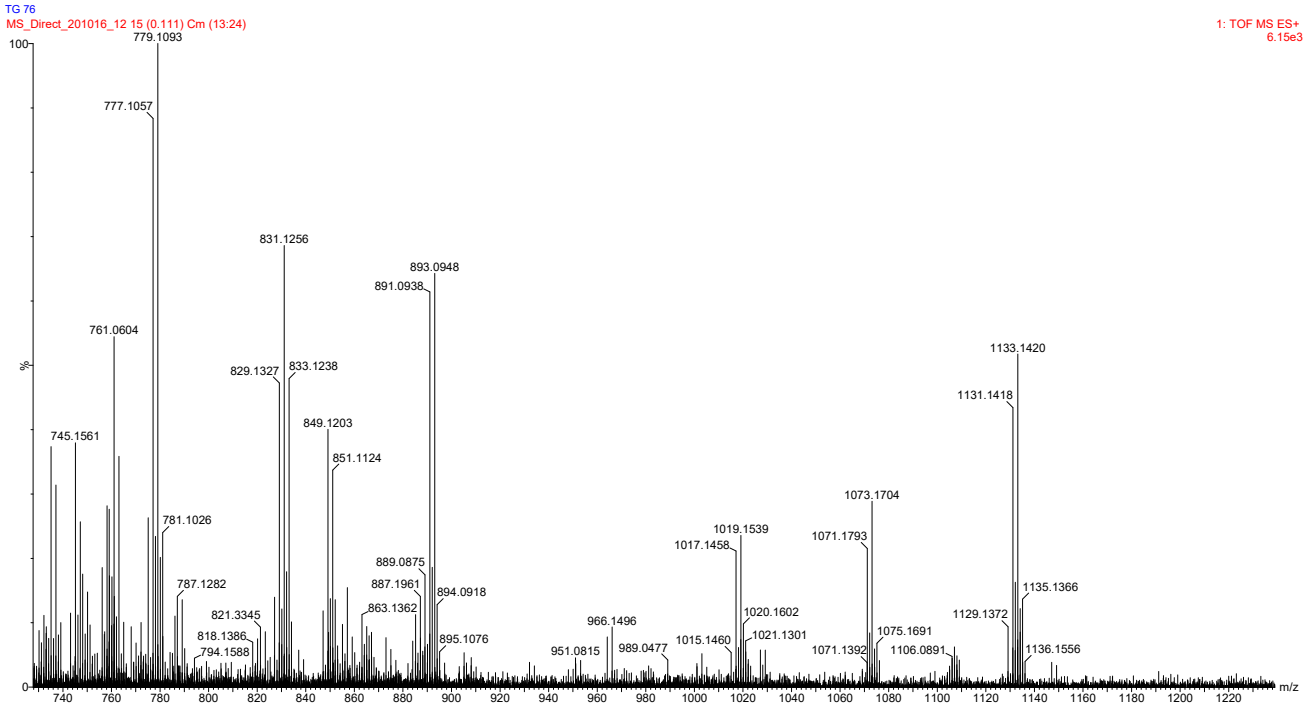

Fig. S31 Mass spectrum of metallarectangle **3c**.

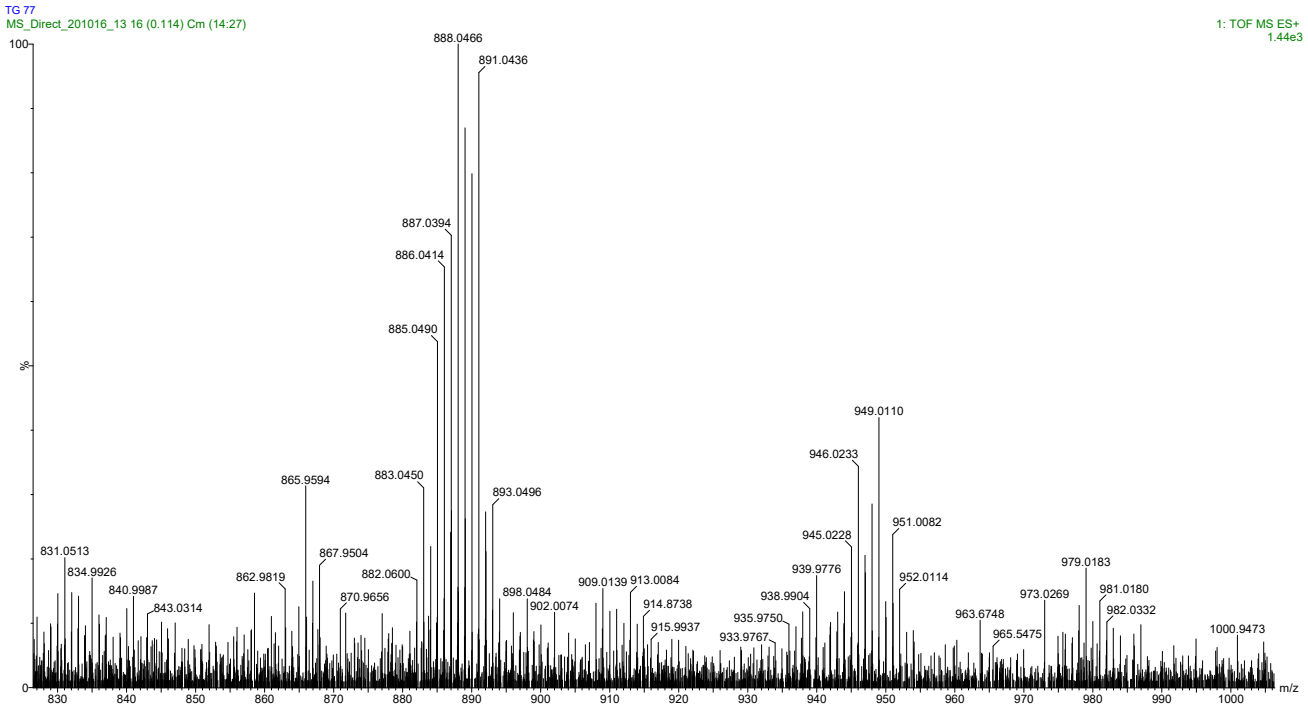

Fig. S32 Mass spectrum of metallarectangle **3d**.

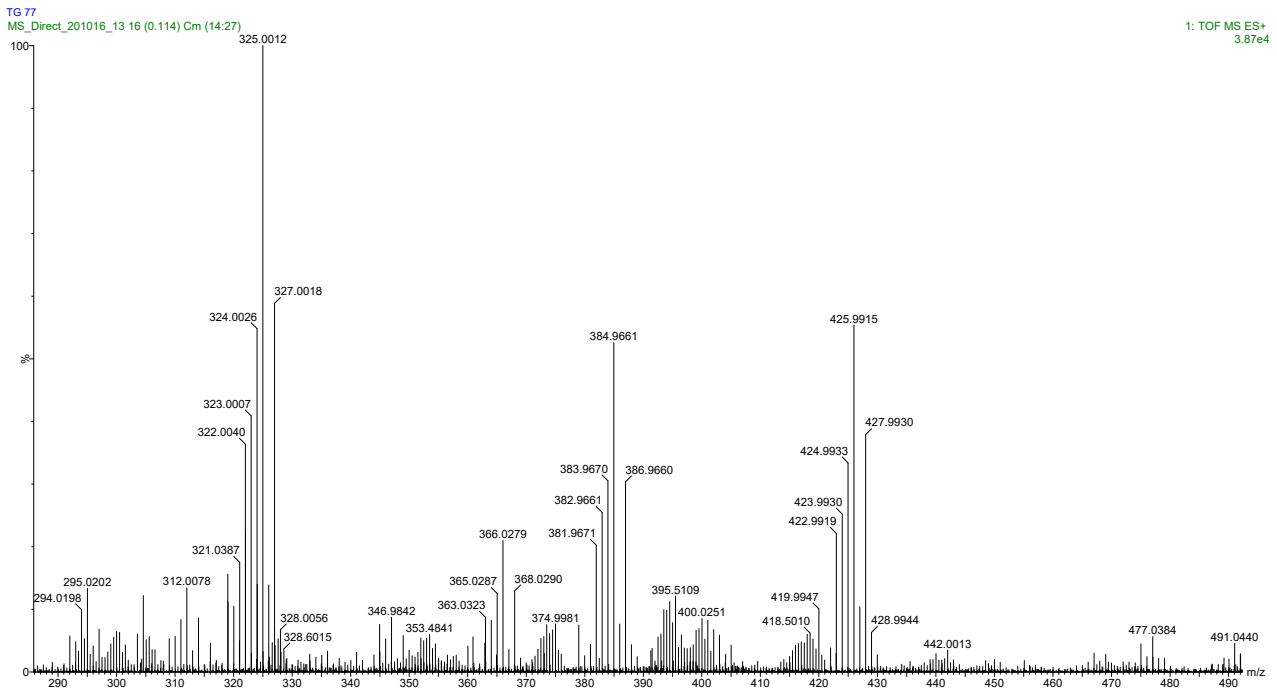

Fig. S33 Mass spectrum of metallarectangle **3d**.